

# Energy dependence of the isomeric cross section ratio in the $^{58}\text{Ni}(n, p)^{58}\text{Co}^{m,g}$ reactions

V. Avrigeanu<sup>1,2</sup>, S. Sudár<sup>2</sup>, Cs. M. Buczkó<sup>2</sup>, J. Csikai<sup>2</sup>, A.A. Filatenkov<sup>3</sup>, S.V. Chuvaev<sup>2,3</sup>,  
R. Dóczy<sup>2</sup>, V. Semkova<sup>2,4</sup>, and V.A. Zelenetsky<sup>5</sup>

<sup>1</sup>*Institute for Physics and Nuclear Engineering, P.O. Box MG-6, 76900 Bucharest, Romania*

<sup>2</sup>*Institut of Experimental Physics, Kossuth University, H-4001 Debrecen, Postfach 105, Hungary*

<sup>3</sup>*V.G. Khlopin Radium Institute, 2nd Murinski Ave. 28, St. Petersburg 194021, Russia*

<sup>4</sup>*Institute of Nuclear Research and Nuclear Energy, 1784 Sofia, Bulgaria*

<sup>5</sup>*Institute of Atomic Energetics, Studgorodok 1, 249020 Obninsk, Russia*

## Abstract

Excitation functions of the  $^{58}\text{Ni}(n, p)^{58}\text{Co}^{m,g}$  reactions were measured in the energy range from 2 to 15 MeV. The energy dependence of the isomeric cross-section ratio  $R = \sigma_m/(\sigma_m + \sigma_g)$  is deduced from the measured data. The shape and magnitude of the  $R(E_n)$  function are described by model calculations using a consistent parameter set. Questions of the input level scheme were solved based on the accurate isomeric ratio measured at low energy region.

PACS number(s): 24.60.Dr, 25.40.-h, 28.20.-v

Typeset using REVTeX

A previous survey of isomeric cross sections pointed out the practical significance of these data in fusion reactor technology as well as in the production of medically important radioisotopes [1]. Furthermore, isomeric cross-section ratios are of basic interest for the analysis of nuclear-spin effect within the formation of isomeric states in nucleon [1] and heavy-ion [2] induced reactions. An illustrative case for the experimental difficulties and the contradictory calculated results is the  $R(E_n)$  function in the case of  $^{58}\text{Ni}(n, p)^{58}\text{Co}^{m,g}$  reactions. Recent measurements and model-calculations [3,4] on the  $R(E_n)$  function have required further investigations to solve the discrepancy in the data [5].

Metallic foils made of enriched  $^{58}\text{Ni}$  and natural Ni were irradiated with neutrons produced via the  $^2\text{H}(d, n)^3\text{He}$  and  $^3\text{H}(d, n)^4\text{He}$  reactions around 2.5 MeV and 14 MeV, respectively. Irradiations were carried out at KRI (St. Petersburg) and IEP (Debrecen) in scattering free arrangements. Neutron flux variation in time and at the sample position was measured in KRI by two independent scintillation detectors. The neutron energy distribution inside samples was calculated by a code taking into account the real experimental conditions such as the size of the beam, the solid angle for the sample, the slowing down and scattering of  $\text{D}^+$  beam in the target.

Usually, the foils were irradiated for 5 h with  $D - D$  and 1 h with  $D - T$  neutrons, respectively. Detection of the 810.8 keV gamma-line was started immediately after irradiation using several detectors simultaneously. Each sample was measured continuously for 2–3 days and the measured spectra were saved in every one or two hours. The intensity of the 810.8 keV gamma-line from the decay of the  $^{58g}\text{Co}$  ground state ( $T_{1/2} = 70.92$  d) populated directly and also by the decay of the  $^{58m}\text{Co}$  isomeric state ( $T_{1/2} = 9.15$  h) was determined as a function of time. These data were compared with the calculated decay curve containing both the  $\sigma_m$  and  $\sigma_g$  parameters. The best values of isomeric ratios were obtained using the weighted least-squares method for the adjustment of the calculated curves to the experimental points.

The uncertainty in the isomeric ratio indicated in Table I was deduced from repeated measurements.

The quasi-monoenergetic neutrons in the 5.38 – 12.38 MeV range were produced by the MGC-20 cyclotron of ATOMKI (Debrecen) using D<sub>2</sub> gas target. The activities of samples were determined by HPGe, NaI and Ge(Li) detectors. Details of the experimental procedures have been published elsewhere [3,6,7]. The measured data are given in Table I. The data points of the  $R(E_n)$  function between 5 and 10 MeV have been deduced from the  $(\sigma_m + \sigma_g)$  and  $\sigma_m$  values measured in KFA (Jülich) by the Co X-rays [8] emitted in the decay of  $^{58}\text{Co}^m$ .

Preequilibrium-emission (PE) and statistical model calculations were carried out by using the computer code STAPRE-H95 [9]. The PE processes have been described by means of the Geometry-Dependent Hybrid (GDH) model including the angular momentum and parity conservation [10,11] which leads to an enhanced PE from higher spin composite-system states and higher orbital momenta in the emergent channels. These aspects are particularly important to our better understanding of the isomeric cross sections [12]). A consistent parameter set, established or validated by means of different types of independent experimental data [11,13] was involved in the GDH calculations. The corresponding discrete level data and level density parameters of the back-shifted Fermi gas (BSFG) model are given in Table II. Particular optical model potential (OMP) parameter sets have been used for neutrons on  $^{58}\text{Ni}$  [14] and  $^{59}\text{Co}$  [15].

The calculated  $R(E_n)$  excitation function obtained by using the evaluated value [16] for the branching ratio of the 52.8 keV→24.9 keV transition is shown in Fig. 1(a). It was found that the calculated cross sections for the  $^{58}\text{Ni}(n,p)^{58}\text{Co}^m$  reaction is lower with  $\sim 35\%$  than the experimental data. As shown in Fig. 1(b) similar behavior can be observed for the  $^{59}\text{Co}(n,2n)^{58}\text{Co}^m$  reaction, in which the same  $^{58}\text{Co}$  residual nucleus is produced.

In order to study the accuracy of the statistical-model calculation, the advantage of the accurate  $R$ -values measured at low energy region was considered [6]. In this case only the statistical population of the lowest few discrete levels and the corresponding decay scheme are important. As shown in Fig. 1(a) by using only the ground and isomeric states the lack of agreement between the experiment and model prediction is gradually corrected for increasing incident energies. This has restricted the possible sources of the underpredicted

values to the decay scheme of the very low-lying levels. It was found that a branching ratio of  $(75\pm 5)\%$  for the  $52.8\text{ keV}\rightarrow 24.9\text{ keV}$  transition brings into agreement the calculated and these particular experimental data. At the same time, the energy dependence of the isomeric cross-section ratio for the  $^{59}\text{Co}(n, 2n)^{58}\text{Co}^{m,g}$  reaction as well as the excitation functions of both the  $^{58}\text{Ni}(n, p)^{58}\text{Co}^{m,g}$  and  $^{59}\text{Co}(n, 2n)^{58}\text{Co}^{m,g}$  reactions are also well reproduced, as shown in Figs. 1(c) and 1(d).

The calculated  $R(E_n)$  excitation function based on the above-mentioned assumption has been tested by an additional analysis of the  $^{58}\text{Co}$  level scheme effect. It should be noted that the most recent evaluation of the level schemes for nuclei with atomic mass  $A=58$  [17] became available when this work was mainly carried out [5]. However, the number of adopted levels of  $^{58}\text{Co}$  corresponding to the excitation energy considered in this work (Table II) was decreased by only one, while the re-evaluated branching ratios using the same experimental data base should be changed also for a single level. In order to check our previous considerations [5] we have used the new evaluation.

The shape of the compound nucleus angular momentum ( $J$ ) distribution given within the statistical model by the neutron OMP [14] is shown in Fig. 2(a). At the lowest incident energies it is bell-like and nearly symmetric at around the average  $\bar{J}$  value (which is, e.g.,  $\sim 2\hbar$  around  $E_n=4\text{ MeV}$ ) and becomes nearly triangular above  $\sim 10\text{ MeV}$ . This distribution may explain the role of various assumptions involved in the case of the adopted levels [16] which have no spin assignment. The question is less severe for such levels which have at least a known branching ratio. The spin values considered for them in the present calculations, marked additionally in Fig. 2(b), are confirmed for two levels by the superseding evaluation [17] and differ by one unit for a third level. The other case happens for three levels, the guidance by the level scheme for  $^{56}\text{Co}$  (with a shell-model configuration having not three but one neutron in the  $p_{3/2}$  shell) being useful only for one of them considered as a  $0^+$  level. The yrast plot has suggested the assignment  $4^+$  for the other two levels of this kind, and we have assumed for them an uniform decay to the ground and isomeric states. This main choice leads to the solid curve in Fig. 1(a), while we have alternatively considered also both

these  $4^+$  levels populating either the ground state (lower dashed curve) or the isomeric state (higher dashed curve). Any other option, e.g. both levels being  $0^+$  or  $6^+$  and decaying only to the g.s. and, respectively, isomeric state, provides  $R(E_n)$  excitation functions between the above-mentioned limits. Therefore, it was found [5] that an uncertainty of about 10% in the isomeric cross-section ratio comes from various spin assignments for only two of the 29 discrete levels of the product nucleus.

The final use of the 28 adopted levels up to 1.555 MeV excitation energy [17] provides an effective check of the above comments. The adoption of the re-evaluated level and decay schemes [17] leads to changes of the calculated  $R(E_n)$  values from  $\sim 3\%$ , around the incident energy of 2 MeV, to  $\sim 0.3\%$  around 14 MeV. On the other hand, the only change of the branching ratios for the third excited level [17] has an enhanced effect on the branching-ratio value of  $(85\pm 5)\%$  for the 52.8 keV  $\rightarrow$  24.9 keV transition which makes possible the agreement between the experimental  $R(E_n)$  data at 2–3 MeV and the calculated results [the solid curve in Fig. 3(a)]. The greatest difference with respect to the calculated  $R(E_n)$  excitation function by using the previous level scheme [16], shown by the solid curve in Fig. 1(a) and dashed curve in Fig. 3(a), is just within the limit of 10% discussed previously.

The meaning of the level schemes of the both residual and competitive reaction channels, for (i) the slope of the calculated  $R(E_n)$  excitation function, and (ii) some "structure" present at the lowest energies (Fig. 3) was analysed. Actually, this (n,p) reaction on an even-even neutron-deficient target nucleus, with a small but positive  $Q$ -value, is a rather particular case. The competition between the even-even  $^{58}\text{Ni}$  and the doubly odd  $^{58}\text{Co}$  residual nuclei should be also carefully considered, especially at lower energies. The analysis illustrated in Fig. 3 makes possible to identify the effect of each of the target-nucleus lowest discrete levels as well as, beyond this behavior, a trend similar to the heavy-ion induced reactions at sub-barrier energies [2] i.e. rather constant  $R$  values just above the reaction threshold. It may also be supported the conclusion [2] that deficient discrete-level schemes used in earlier analyses require a nuclear moment of inertia lower – typically one-half – as the rigid-body value  $I_r$  (with reduced radius  $r_0=1.25$  fm) in order to reproduce the measured  $R$  data.

Actually, it was shown that there is no reduction of the effective moment of inertia below the rigid body value, e.g., by Fisher *et al.* [18] through study of the spin cut-off parameters for  $^{53}\text{Cr}$  and  $^{57}\text{Fe}$  derived from analysis of neutron-induced reactions at 14.1 MeV; this result was next successfully used by the same group of IRK-Vienna for description of the all neutron reactions on  $^{58}\text{Ni}$  up to 20 MeV [19], and in subsequent calculations in the range  $A=46-64$  [11,13].

Calculation of the  $R(E_n)$  excitation function has been carried out by using the assumption of the one-half rigid body value for the nuclear moment of inertia. The corresponding other two BSFG parameters have been obtained by the fit of the same discrete level data (Table II). However, the calculated isomeric cross-section ratio does not depend on the nuclear level density for incident energies lower than  $\sim 3.5$  MeV. Above this energy up to 15 MeV the calculated values by using  $0.5I_r$  are lower, and can achieve about 12% at the highest energy, with respect to the solid curve in Fig. 1(a). Except the better agreement with the three experimental data around 12 MeV, this assumption leads to worse description of data especially around 14 MeV. In conclusion one can say that neither the uncertainty in the level scheme at higher energies nor the level density parameters have a significant effect on this analysis, based on the precise experimental data at low energies. Further analysis is required for the other reactions involved [4] in the study of this isomeric cross-section ratio especially at higher incident energies where the model calculation need additional improvement [24].

## ACKNOWLEDGEMENTS

This work was supported in part by the Hungarian Research Found (Contract No. T 025024), the International Atomic Energy Agency, Vienna (Contract Nos. 7687/R0 and 8205), the International Science and Technology Center (Project No. 176), and the Romanian Ministry of Research and Technology Grant No. 3028GR/B10.

## References

- [1] S.M. Qaim, *Nuclear Data for Science and Technology*, edited by J.K. Dickens (ANS, La Grange Park, 1994), p. 186.
- [2] D.E. DiGregorio, K.T. Lesko, B.A. Harmon, E.B. Norman, J. Pouliot, B. Sur, Y. Chan, and R.G. Stokstad, *Phys. Rev. C* **42**, 2108 (1990); O.A. Capurro, D.E. DiGregorio, S. Gil, D. Abriola, M. di Tada, J.O. Fernández Niello, A.O. Macchiavelli, G.V. Martí, A.J. Pacheco, J.E. Testoni, D. Tomasi, and I. Urteaga, *Phys. Rev. C* **55**, 766 (1997).
- [3] Cs.M. Buczkó, J. Csikai, S. Sudár, Á. Grallert, S.A. Jonah, B.W. Jimba, T. Chimoye, and M. Wagner, *Phys. Rev. C* **52**, 1940 (1995).
- [4] S. Sudár and S.M. Qaim, *Phys. Rev. C* **53**, 2885 (1996).
- [5] V. Avrigeanu, S. Sudár, Cs.M. Buczkó, J. Csikai, A.A. Filatenkov, S.V. Chuvaev, R. Dóczy, V. Semkova, and V.A. Zelenetsky, *Nuclear Data for Science and Technology*, edited by G. Reffo, A. Ventura, and C. Grandi (Editrice Compositori, Bologna, 1997), p. 1274.
- [6] A.A. Filatenkov, S.V. Chuvaev, V.N. Aksenov, and V.A. Jakovlev, International Atomic Energy Agency, Report INDC(CCP)-402, Vienna, 1997.
- [7] A.A. Filatenkov, S.V. Chuvaev, V.A. Jakovlev, and V.P. Popik, *Fusion Eng. and Design* **37**, 151 (1997).
- [8] S. Sudár, J. Csikai, S.M. Qaim and G. Stöcklin, *Nuclear Data for Science and Technology*, edited by S.M. Qaim (Springer-Verlag, Berlin, 1991), p. 291.
- [9] M. Uhl and B. Strohmaier, Institut für Radiumforschung und Kernphysik, Report IRK 76/01, Vienna, 1976; M. Avrigeanu and V. Avrigeanu, Institute of Physics and Nuclear Engineering, Report NP-88-1995, Bucharest, 1995.
- [10] M. Avrigeanu, M. Ivaşcu, and V. Avrigeanu, *Z. Phys. A* **329**, 177 (1988); *Rev. Roum.*

- Phys. **32**, 697 (1987).
- [11] M. Avrigeanu, M. Ivaşcu, and V. Avrigeanu, Z. Phys. A **335**, 299 (1990); V. Avrigeanu, Rev. Roum. Phys. **37**, 139 (1992).
- [12] H.H. Bissem, W. Scobel, J. Ernst, M. Kaba, J. Rama Rao, and H. Strohe, Phys. Rev. C **22**, 1468 (1980).
- [13] M. Avrigeanu and V. Avrigeanu, J. Phys. G **20**, 613 (1994); M. Avrigeanu, A. Harangozo, and V. Avrigeanu, Rom. J. Phys. **41**, 77 (1996).
- [14] S. Chiba, P.T. Guenther, R.D. Lawson, and A.B. Smith, International Atomic Energy Agency, Report No. INDC(NDS)-247, Vienna, 1991, p.7.
- [15] A.B. Smith and R.D. Lawson, Nucl. Phys. **A483**, 50 (1988).
- [16] L.K. Peker, Nucl. Data Sheets **61**, 189 (1990).
- [17] M.R. Bhat, Nucl. Data Sheets **80**, 789 (1997).
- [18] R. Fisher, G. Traxler, M. Uhl, and H. Vonach, Phys. Rev. C **30**, 72 (1984).
- [19] A. Pavlik, G. Winkler, M. Uhl, A. Paulsen, and H. Liskien, Nucl. Sci. Eng. **90**, 186 (1985).
- [20] A.H. Wapstra and G. Audi, Nucl. Phys. **A432**, 55 (1985).
- [21] C.M. Baglin, Nucl. Data Sheets **69**, 733 (1993).
- [22] H. Junde, Nucl. Data Sheets **64**, 723 (1991).
- [23] H. Vonach, M. Uhl, B. Strohmaier, B.W. Smith, E.G. Bilpuch, and G.E. Mitchell, Phys. Rev. C **38**, 2541 (1988).
- [24] A. Fessler, E. Wattercams, D.L. Smith and S.M. Qaim, Phys. Rev. C **58**, 996 (1998).



TABLE I. Measured cross sections for the  $^{58}\text{Ni}(n,p)^{58}\text{Co}$  and  $^{58}\text{Ni}(n,p)^{58}\text{Co}^m$  reactions, and measured and deduced isomeric cross section ratios for the former reaction.

Neutron energy (MeV)	Measured $\sigma(n,p)$ (mb)	Measured $\sigma_m$ (mb)	Measured $\sigma_m/(\sigma_g + \sigma_m)$	Deduced
2.14		19.2±1.3	0.260±0.014	
2.21			0.259±0.011	
2.23			0.274±0.026	
2.30		20.6±1.4	0.234±0.010	
2.43			0.254±0.012	
2.59			0.277±0.011	
2.60		29.1±2.0		
2.74		41.0±3.0	0.289±0.012	
2.83			0.269±0.008	
2.84			0.278±0.009	
2.94		56.3±3.5	0.276±0.011	
10.3			0.445±0.019	
12.3			0.452±0.020	
13.4			0.545±0.004	
13.56	413.6±13.2	234±9		0.566±0.028
13.6			0.536±0.004	
13.74	383.4±16.1	218±9		0.569±0.034
13.96	359.1±17.2	197±8		0.549±0.035
14.03			0.545±0.007	
14.05			0.552±0.005	
14.19	329.9±12.8	182±8		0.552±0.032
14.42	313.8±10.8	170±7		0.542±0.029
14.48			0.573±0.012	
14.61	292.3±14.0	173±11		0.592±0.047
14.68			0.556±0.006	
14.78	275.9±11.8	150±6		0.544±0.032
14.88			0.573±0.005	

TABLE II. The number of discrete levels  $N_d$  up to excitation energy  $E_d$  used in Hauser–Feshbach calculations, taken from the corresponding references, and the low–lying levels as well as s–wave nucleon–resonance spacings  $\overline{D}_{exp}$  in the nucleon energy range  $\Delta E$  above the corresponding binding energy  $B_n$  [20] used to obtain the BSFG parameters, i.e. the level–density parameter  $a$ , the ratio of the nuclear moment of inertia  $I/I_r$ , and the ground–state shift  $\Delta$ .

Nucleus	$N_d$	$E_d$ (MeV)	Ref.	Fitted level and resonance data				$a$ (MeV <sup>-1</sup> )	$I/I_r$	$\Delta$ (MeV)
				$N_d$	$E_d$	$B_n + \frac{\Delta E}{2}$	$\overline{D}_{exp}$			
					(MeV)	(MeV)	(keV)			
<sup>59</sup> Ni	13	1.948	[21]	20	2.48	9.33	12.5±0.9 <sup>a</sup>	6.25	1.0	-1.20
<sup>58</sup> Ni	28	4.475	[17]	32	4.58			6.00	1.0	0.28
<sup>58</sup> Co	28	1.555	[17]	28	1.56			6.60	1.0	-2.37
<sup>58</sup> Co	28	1.555	[17]	28	1.56			6.11	0.5	-2.40
<sup>55</sup> Fe	16	2.600	[22]	16	2.60	9.55	18.0±2.4 <sup>a</sup>	5.60	1.0	-1.30

<sup>a</sup>Reference [23].

## FIGURE CAPTIONS

FIG. 1. Comparison of the measured and calculated excitation functions and isomeric cross section ratios for the  $^{58}\text{Ni}(n, p)^{58}\text{Co}^{m,g}$  and  $^{59}\text{Co}(n, 2n)^{58}\text{Co}^{m,g}$  reactions. The calculated cross-section curves (c),(d) were obtained by using the fitted value of the branching ratio for the 52.8 keV $\rightarrow$ 24.9 keV transition (solid curves), the isomeric cross-section ratios (a),(b) were found by using also the evaluated branching-ratio [16] (dotted curves), using only the two levels (dashed-dotted curves), as well as the fitted branching-ratio but considering two assigned  $4^+$  levels populating either the g.s. (lower dashed curves) or the isomeric state (higher dashed curves). For the experimental data see Refs. [3,4].

FIG. 2. (a) Partial cross sections for the compound nucleus formation versus the corresponding total angular momentum  $J_{CN}$ , at the given incident energies of neutrons on the target nucleus  $^{58}\text{Ni}$ . (b) The yrast plot for the residual nucleus  $^{58}\text{Co}$ , of the adopted discrete levels [16] including the spin assignment (+), while in the opposite case the spin values considered in the present calculations are additionally marked if the corresponding level has an adopted decay scheme ( $\times$ ) or only the excitation energy ( $\circ$ ); the yrast lines showed only for orientation correspond [9,10] to the effective excitation energies obtained by using the BSFG parameters in Table II, and the nuclear moment of inertia for a rigid body  $I_r$  (dashed curve) and respectively one-half of  $I_r$  (dotted curve) with a reduced radius  $r_0=1.25$  fm.

FIG. 3. The same as Fig. 1(a), except the calculated values are obtained by using (a) 28 discrete levels up to the excitation energy  $E^*=4.475$  MeV of the nucleus  $^{58}\text{Ni}$ , while for the nucleus  $^{58}\text{Co}$  are used either 28 discrete levels [17] (solid curve) or 29 levels [16] (dashed curve) up to  $E^*=1.555$  MeV, 3 discrete levels up to  $E^*=0.053$  MeV (dotted curve), or 2 discrete levels up to  $E^*=0.025$  MeV (dashed-dotted curve), and (b) only 2 discrete levels up to  $E^*=0.025$  MeV for the nucleus  $^{58}\text{Co}$  while for the nucleus  $^{58}\text{Ni}$  are used either 28 levels up to  $E^*=4.475$  MeV (solid curve), only g.s. (dashed curve), 2 levels up to  $E^*=1.454$  MeV (dashed-dotted curve), or 4 levels up to  $E^*=2.776$  MeV (dotted curve).

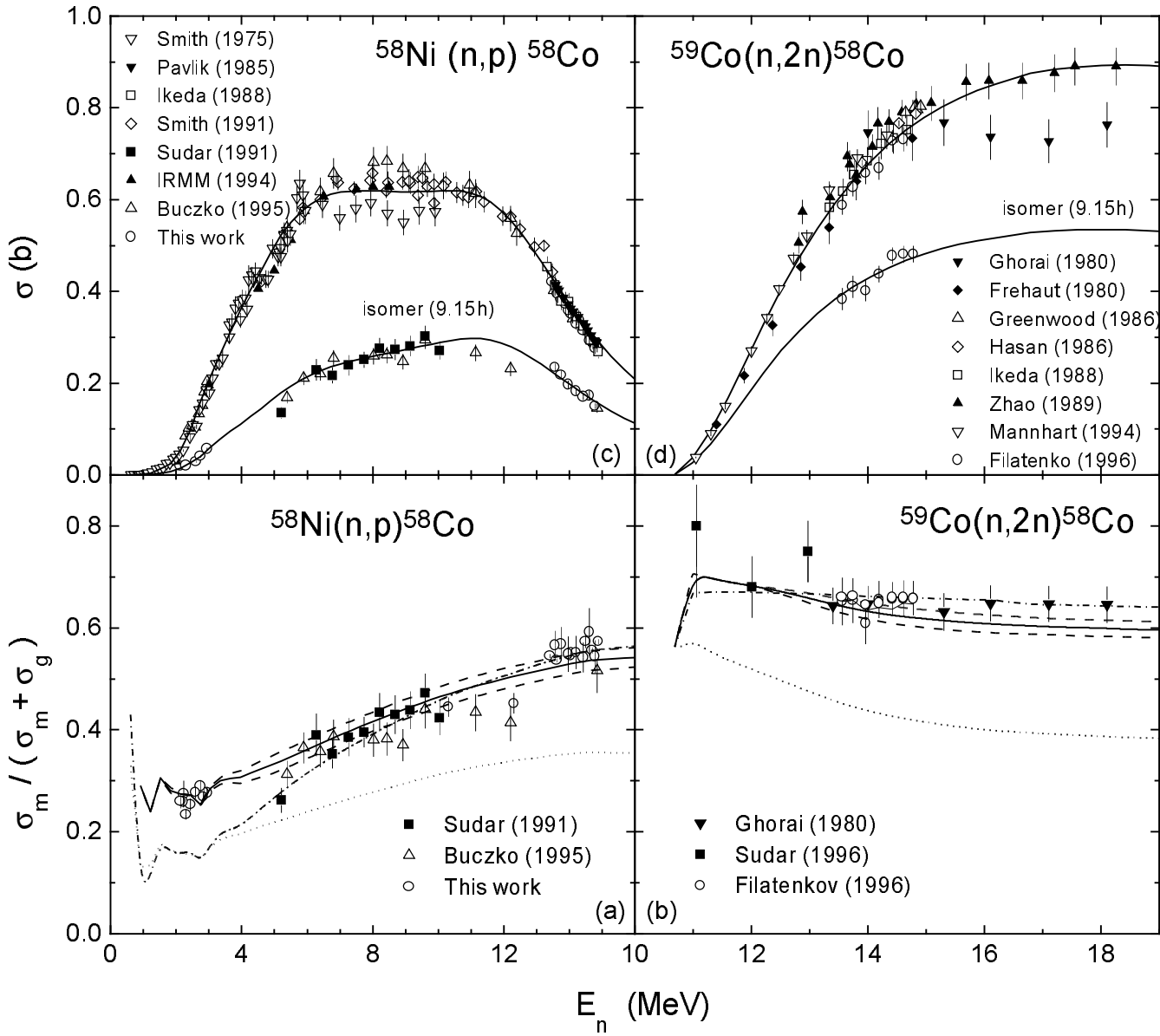


Fig. 1. - V. Avrigeanu et al.

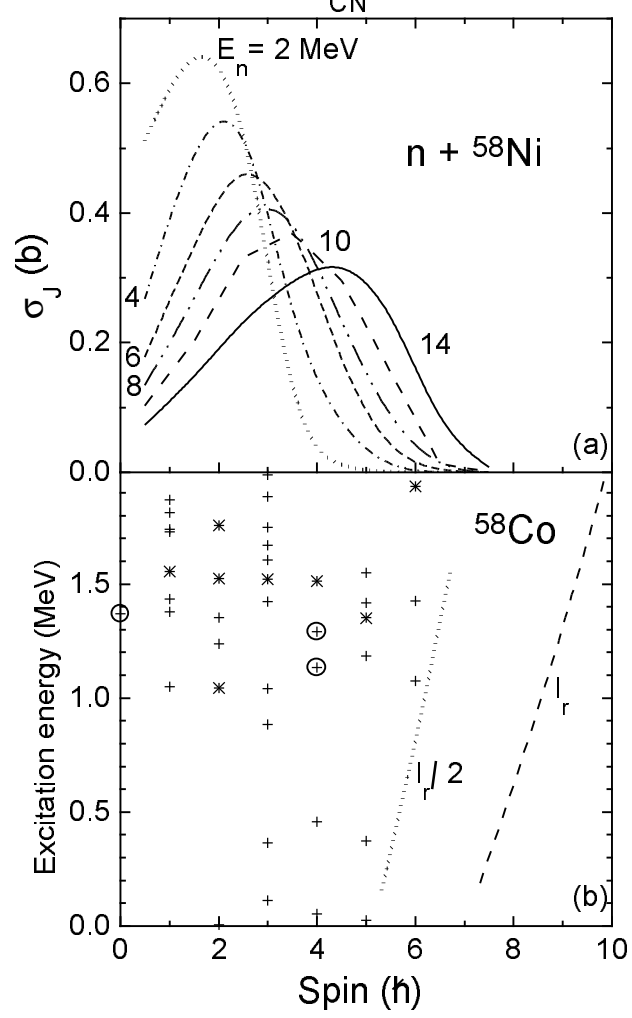


Fig. 2. - V. Avrigeanu et al.

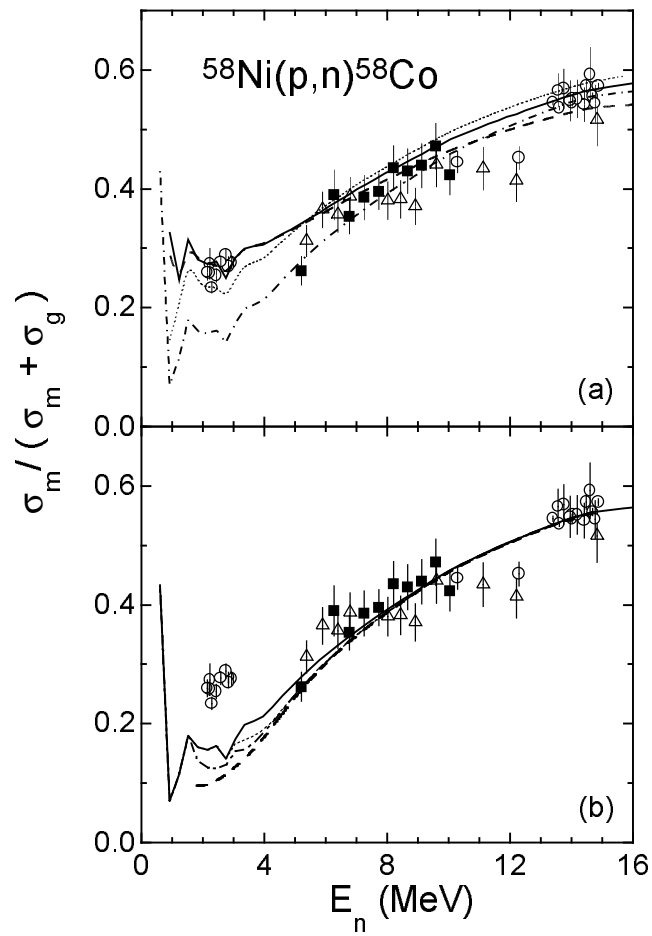


Fig. 3. - V. Avrigeanu et al.